Int J Clin Exp Med 2025;18(12):288-300
www.ijcem.com /ISSN:1940-5901/IJCEM0167240

Original Article

CD36 promotes chemotherapy resistance and stemness of cervical cancer cells through the Hippo and ERK5 pathway activation

Lin-Ying Xie[1*], Zi-Gui Chen[2,3*], Ya-Li Xiang[1], Chao Zeng[1]

[1]Department of Pathology, The Eighth Affiliated Hospital, Sun Yat-sen University, Shenzhen 518033, Guangdong, China; [2]Department of Pathology, Shenzhen Luohu Hospital of Traditional Chinese Medicine, Shenzhen 518001, Guangdong, China; [3]Department of Pathology, Shenzhen Hospital Shanghai University of Traditional Chinese Medicine, Shenzhen 518001, Guangdong, China. [*]Equal contributors.

Received July 4, 2025; Accepted October 28, 2025; Epub December 15, 2025; Published December 30, 2025

Abstract: Objectives: Our previous work revealed that CD36 accelerates the progression of cervical cancer. Here, we elucidate the role of CD36 in regulating stemness and chemotherapy resistance in cervical cancer cells. Methods: Bioinformatic analysis was used to assess the correlation between CD36 expression and chemotherapy drug sensitivity in advanced cervical cancer. The effects of CD36 on cell proliferation were evaluated using Cell Counting Kit-8 and colony formation assays. Tumorsphere formation assays were performed to assess stemness. Western blot analysis was conducted to examine correlations between CD36 expression and stem cell markers. Chemotherapy resistance was further evaluated using colony formation, Cell Counting Kit-8 assays, and flow cytometry. Finally, the molecular mechanisms by which CD36 influences stemness and resistance were explored through bioinformatics analysis and western blotting. Results: CD36 expression was positively correlated with cisplatin resistance in advanced cervical cancer. CD36 overexpression enhanced both stemness and chemotherapy resistance. Notably, CD44, Hippo, and MEK5/ERK5 pathways were implicated in CD36-mediated effects. Conclusion: CD36 may serve as an effective therapeutic target to improve the prognosis of cervical cancer.

Keywords: CD36, stemness, chemotherapy resistance, cervical cancer

Introduction

Cervical cancer is the most common malignancy of the female genital tract [1]. Its progression involves infection with human papillomavirus, cervical intraepithelial neoplasia, local invasion, and metastasis [2, 3]. Widespread use of cytological screening and biopsies has effectively reduced cervical cancer incidence. However, advanced cervical cancer continues to have a poor prognosis due to chemotherapy resistance [4]. Therefore, elucidating the mechanisms underlying chemotherapy resistance in cervical cancer is essential.

Cancer cells use fatty acids as an energy source to reprogram metabolism. CD36, a lipid transporter, is a membrane protein expressed on monocytes, epithelial cells, and endothelial cells [5-8]. In cancer cells, CD36 overexpression accelerates fatty acid uptake and lipid accumulation, promoting growth and metastasis [9-12]. Lipid accumulation also exerts immunosuppressive effects [13]. Owing to its multifaceted roles in cancer biology, CD36 has recently emerged as a promising therapeutic target in various cancers [14-18]. Notably, silencing CD36 inhibits clonogenicity and stemness marker expression in bladder cancer cells, highlighting its critical role in enhancing stemness properties [19]. However, current understanding of CD36's role in regulating stemness and chemotherapy resistance in cervical cancer cells remains limited.

Cancer stem cells (CSCs) are tumor-initiating cells that are capable of differentiating into multiple cell types and contributing to tumorigenicity and chemotherapy resistance in solid malignancies [20-22]. However, limited studies have examined the relationship between cervical CSCs, chemotherapy resistance, and can-

https://doi.org/10.62347/HFTC6895

cer progression. CD44, a cervical tumorigenesis stem cell marker, can enhance CSC self-renewal and chemotherapy resistance [23]. Yes-associated protein (YAP) promotes malignant transformation of cervical intraepithelial neoplasia by reinforcing CSC traits [24]. In this study, we explored the roles of CD36 in regulating stemness and chemotherapy resistance in cervical cancer cells. Further, we investigated the specific mechanisms through which CD36 facilitates these processes.

Materials and methods

Acquisition of cervical cancer transcriptome data

We downloaded transcriptome sequencing data (ribonucleic acid [RNA] sequencing) for cervical cancer from The Cancer Genome Atlas database (https://www.cancer.gov/ccg/research/genome-sequencing/tcga) using the Illumina HiSeq 2000 platform. The dataset included 62 advanced cervical cancer samples (41 stage 4 and 21 additional stage 4 cases). Details of the downloaded data are provided in Table S1. This study was approved by the ethics committee of the Eighth Affiliated Hospital of Sun Yat-Sen University.

Half-maximal inhibitory concentration (IC_{50}) correlation analysis

CD36 expression levels in cervical cancer specimens from The Cancer Genome Atlas database were analyzed in combination with data from the Genomics of Drug Sensitivity in Cancer database (https://www.cancerrxgene.org/) [25]. The R version 4.3.1 pRRophetic package (https://github.com/paulgeeleher/pRRophetic) was used to evaluate the sensitivity of advanced cervical cancer to various chemotherapeutic agents [26]. Using the downloaded drug data as a reference, the pRRophetic package estimated the IC_{50} value of each sample based on whole-genome expression.

Kyoto encyclopedia of genes and genomes pathways analysis

The correlation between CD36 gene expression and all of the other genes was calculated in 62 advanced cervical cancer samples using the Pearson correlation coefficient. Genes with correlation coefficients above 0.3 and *P*-values below 0.05 were retained. The Database for Annotation, Visualization and Integrated Discovery (DAVID) version 6.8 (https://david.ncifcrf.gov/) was then used to perform Kyoto Encyclopedia of Genes and Genomes (KEGG) pathway enrichment analysis on the selected genes, applying a *P*-value threshold of less than 0.05 [27]. There were 10 KEGG pathways that met the significance criteria.

Prognostic analysis

For prognostic analysis, the R version 4.3.1 survival package (version 2.41-1; https://cran.r-project.org/web/packages/finalfit/vignettes/survival.html) was used to evaluate the correlation between CD36 expression and prognosis in advanced cervical cancer [28]. The effects of CD36 expression and clinical stage on patient prognosis were analyzed.

Cell culture

C33a and HeLa cells were obtained from the Type Collection Center (Wuhan, China) and cultured in Dulbecco's Modified Eagle Medium (Gibco, CA, USA). C33a cells were incubated with fluorescein isothiocyanate-labeled CD133 and sorted by flow cytometry. The CD133-positive C33a cell population was collected, expanded, and cultured *in vitro* as C33a-Cervical CSCs (C33a-CCSCs).

Plasmid construction and transfection

The pIRES2-ZsGreen1-CD36 plasmid, designed to overexpress CD36, was constructed by cloning the CD36 coding sequence into the pIRES2-ZsGreen1 vector. C33a-CCSCs were transfected with the plasmid using Lipo™6000 (Beyotime, Shanghai, China) and selected in medium containing 600 μg/ml G418 for three weeks. The empty pIRES2-ZsGreen1-NC plasmid served as a negative control (NC). CD36-overexpressing C33a and C33a-CCSCs cells were designated as "C33a/CD36" and "C33a-CCSCs/CD36", respectively.

Transfection with siRNA (small interfering RNA)

Human CD36 small interfering ribonucleic acid (siRNA) was purchased from Guangzhou Ribo (Guangzhou, China). Cells were seeded in six-well plates at a density of 2×10^5 cells/well. HeLa cells were transfected with CD36 siRNA (HeLa/siRNA CD36) (sense: 5'-CCUGAUAGAAAUGAUCUUATT-3'; antisense: 5'-UAAGAUCAUUU-

CUAUCA GGTT-3') or NC siRNA (HeLa/NC-siRNA) (sense: 5'-UUCUCCGAACGUGUCACGUTT-3'; antisense: 5'-ACGUGACACGUUCGGAGAATT-3') using Lipo™3000 (Thermo Fisher Scientific, Waltham, USA) at a final concentration of 100 nM.

Flow cytometry analysis of the ratios of CD133 positive cervical cancer cells

C33a/CD36 and HeLa/CD36-siRNA cells were centrifuged at 1500 rpm for 5 min. The cells were resuspended in 200 µl of phosphate-buffered saline, followed by the addition of 5 µl of CD133 antibody to each flow tube. Samples were incubated at 4°C for 30 min. After adding another 200 µl of phosphate-buffered saline, the proportion of CD133-positive cells was analyzed by flow cytometry.

Tumorsphere formation assay

C33a/CD36, C33a-CCSCs/CD36, or HeLa/siRNA CD36 cells were incubated in Dulbecco's Modified Eagle Medium supplemented with 20 ng/ml basic fibroblast growth factor, 20 ng/ml epidermal growth factor, and 1 × B27. Cells were seeded in low-attachment six-well plates at a density of 2×10^4 cells/well and cultured for 10 days. Three fields were randomly selected from confocal images, and the number of stem cell spheres with diameters greater than 100 µm was counted for each group.

Western blot

After boiling for 8 min, total protein (80 µg) was loaded onto a 10% polyacrylamide gel and transferred to a polyvinylidene fluoride membrane. The membrane was incubated with the following primary antibodies: CD36 (1:1000; Ab252923, Abcam, Cambridge, UK), CD44 (1:3000; A19020, Abclonal, MA, USA), CD133 (1:1000; AF5120, Affinity, Cincinnati, USA), Nanog (1:5000; 67255-1-Ig, Sanying, Wuhan, China), YAP (1:1000; AF6328, Affinity, Cincinnati, USA), TAZ (1:300; A8202, Abclonal, MA, USA), Bcl-2 (1:3000; 26593-1-AP, Sanying, Wuhan, China), Bax (1:10000; 60627-1-Ig, Sanying, Wuhan, China), MEK5 (1:2000; DF7667, Affinity, Cincinnati, USA), ERK5 (1:1000; DF6835, Affinity, Cincinnati, USA), cleaved caspase-3 (1:1000; AF7022, Affinity, Cincinnati, USA), and GAPDH (1:1000; ABP-R001, Xianzhi Biology, Hangzhou, China). Membranes were then incubated with horseradish peroxidase-conjugated secondary antibodies (1:10000; BA1051, BA1054; Boster Biology, Wuhan, China). Proteins were visualized using a chemiluminescence kit (Pierce; Thermo Fisher Scientific, Inc., Massachusetts, USA).

Colony formation assay

HeLa/siRNA CD36, HeLa/NC siRNA, and HeLa cells were seeded at 200 cells/well in six-well plates [29]. The cells were incubated at 5% CO_2. After 14 days, colonies were stained with trypan blue, and the number of cell colonies was counted.

CCK8 *assay*

C33a/CD36, C33a-CCSCs, HeLa/siRNA CD36 cells and the corresponding control groups were inserted into 96-well plates with 5×10^3 cells per well and cultured 24h at 37°C. 10 µl CCK8 per well were added and cultured at 37°C for 2 h. The absorbance value OD450 of each well was determined by microplate reader. Cell survival rate %= [(experimental hole absorbance) - (blank hole absorbance)]/[control hole absorbance) - (blank hole absorbance)] ×100%.

TUNEL assay

C33a-CCSCs, C33a-CCSCs/CD36 and C33a-CCSCs/NC were seeded at a density of 4×10^5 cells/well in six-well plates. After added 0.5 ml fixative, the cells were permeabilized by 0.2% Triton X-100. Removed the excess PBS, 100 µl of TUNEL equilibrium solution was added to each sample. A TUNEL reaction mixture containing TdT enzyme and fluorescein-dUTP was applied and incubated at 37°C for 2 h. Then diluted DAPI was added, and the samples were further incubated at room temperature for 5 min. The samples were observed under a fluorescence microscope.

Immunofluorescence

After the tissue sections were deparaffinized, antigen repair was performed. After blocking non-specific binding with 5% diluted goat serum, sections were incubated with primary antibodies against CD44 (dilution, 1:100; A19020, Abclonal, MA, USA) and CD133 (dilution, 1:100; AF5120, Affinity, Cincinnati, USA) at 4°C overnight, then incubated with secondary antibody (dilution, 1:100; BA1105,

BOSTER, Wuhan, China). Nuclei were stained by 4',6- Diamidino-2-phenylindole (DAPI). After using anti-fluorescence quencher, the images were observed under a fluorescence microscope. Image-Pro Plus 6.0 software (Media Cybernetics,Maryland, USA) was used to quantitatively analyze the expressions of CD133 and CD44 in each group. The mean optical density value represents the protein expression level.

Flow cytometry analysis of apoptosis

Cells were centrifuged at 1500 rpm for 5 min. The ratios of apoptotic in cervical cancer cells were measured using Annexin V FITC/PI Apoptosis Detection Kit.

Animal assay

Four-week-old female BALB/C nude mice were purchased from SiBei Fu Animal Center (Beijing, China). C33a/CD36 cells (2×10^6/mL) were injected subcutaneously into the axilla of the right forelimb of nude mice. Each group had six nude mice. In vivo imaging detection was performed with a small animal in vivo imager (IVIS Lumina III, Perkin Elmer). We euthanized the nude mice with anesthesia. The nude mice were housed in an animal room with a temperature of 25°C and humidity levels ranging from 40 to 60%. The animal experiment protocol was carried out in accordance with the regulations of the Institutional Animal Ethical Care Committee of the Eighth Affiliated Hospital, Sun Yat-sen University.

Statistical analysis

Data are presented as mean ± standard error of the mean (SEM). The overall survival rate was calculated by plotting the survival curve with the Kaplan-Meier method. Statistical comparisons of data from the experiments on cultured cells or mice were performed using the two-tailed Student's *t* test. All of the statistical analyses were performed using Statistical Package for the Social Sciences version 17.0 (SPSS Inc., Chicago, USA). Differences were considered significant when the *p* value < 0.05.

Results

Correlation between CD36 expression level and resistance of chemotherapy drugs in advanced cervical cancer

The IC_{50} value reflects the sensitivity of chemotherapeutic drugs, and its correlation with CD36 expression was evaluated through bioinformatic analysis (Table S2). Notably, higher CD36 expression in advanced cervical cancer was associated with increased IC_{50} values for cisplatin. Additionally, CD36 expression showed a positive correlation with cisplatin resistance and a negative correlation with vinorelbine resistance in advanced cervical cancer (**Figure 1A**).

Analysis of downstream pathways regulated by CD36 in advanced cervical cancer

In 62 advanced cervical cancer samples, 648 genes were identified as significantly associated with CD36 expression (Table S3). KEGG pathway enrichment analysis was conducted using DAVID version 6.8. There were 10 KEGG pathways that were identified based on a *P*-value threshold of <0.05 (**Figure 1B**). Among these, the Hippo and MEK5/ERK5 signaling pathways were associated with chemotherapy resistance and cancer cell stemness. However, no correlation was observed between CD36 expression and prognosis in patients with advanced cervical cancer (**Figure 1C-F**). CD36 expression was positively correlated with the expression of CD44, CD133, YAP, TAZ, MEK5, and ERK5 in cervical cancer cells (**Figure 1G-J**). These results suggest that CD36 may enhance stem cell marker expression and activate the Hippo and MEK5/ERK5 pathways *in vitro*.

CD36 promotes stemness and tumor growth in vivo

After six weeks, CD36 overexpression significantly promoted tumor growth in female BALB/c-nu mice compared with the C33a/Con group (1636.12 ± 462.29 mm^3 *versus* 732.64 ± 329.89 mm^3; **Figure 2A-C**). Additionally, immunofluorescence assays showed that CD133 (mean optical density: 0.81 ± 0.04 *versus* 0.31 ± 0.01; **Figure 2D**) and CD44 expression (0.95 ± 0.05 *versus* 0.48 ± 0.03; **Figure 2E**) were increased in the C33a/CD36 group compared to controls. These findings suggest that CD36 may promote cervical cancer cell growth by enhancing stemness *in vivo*.

CD36 promoted the stemness of cervical cancer cells in vitro

As shown in **Figure 3A**, **3B**, the number of stem cell spheres with diameters greater than 100 μm was higher in the C33a/CD36 group (5.33 ± 0.58) than in the C33a/NC group (1.67 ±

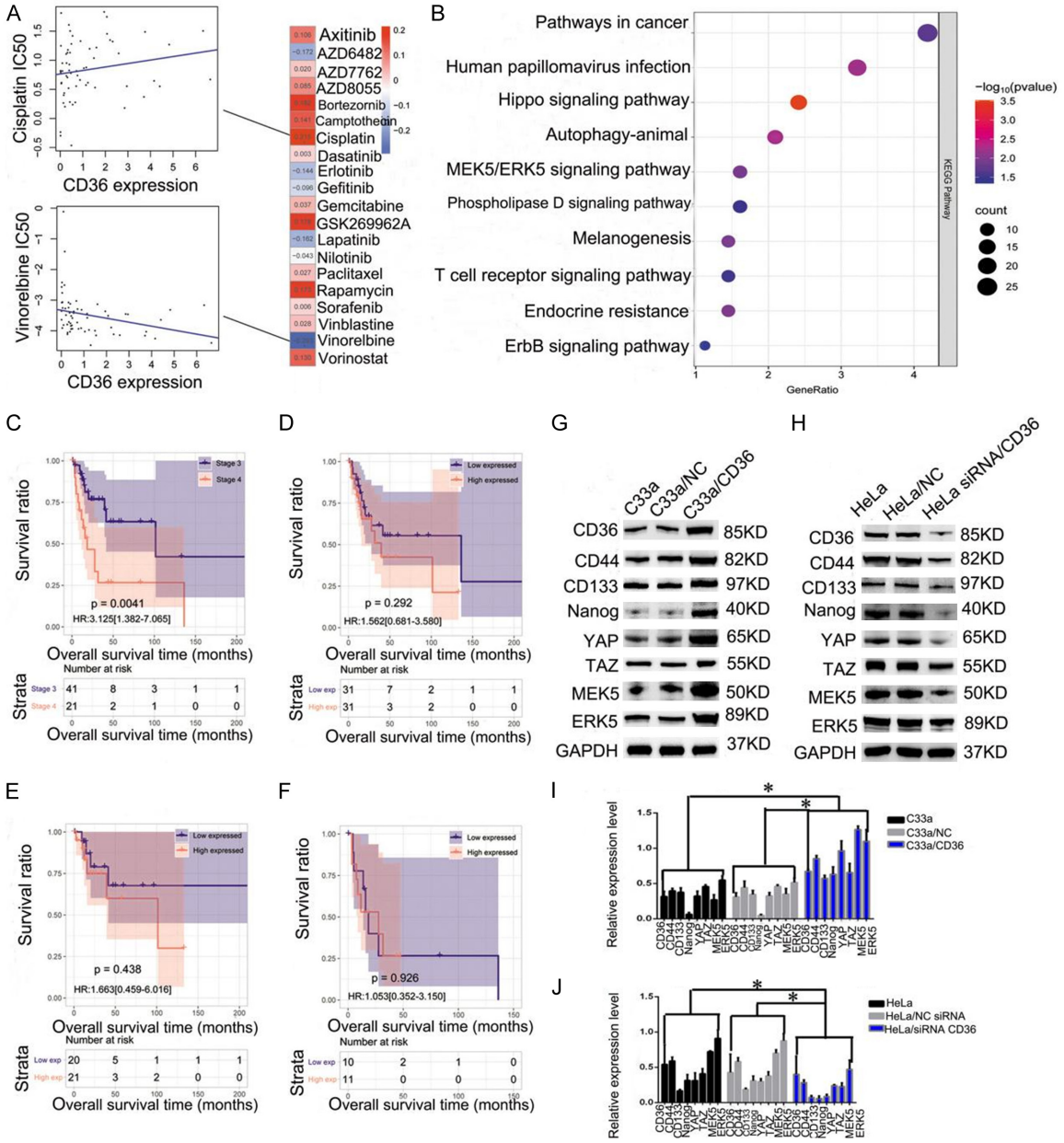

Figure 1. Correlation between CD36 expression and resistance to chemotherapy drugs and prognosis of cervical cancer and its regulated signaling pathways. A: CD36 expression had the most significant positive correlation with cisplatin resistance and the most significant negative correlation with vinorelbine in advanced cervical cancer by IC_{50} correlation analysis. Scale represents *P* value. B: KEGG analysis downstream pathways regulated by CD36 in advanced cervical cancer. C: Kaplan-Meier analysis showed the prognosis of stage 3 cervical cancer was significantly better than stage 4 cervical cancer. D: Kaplan-Meier analysis showed CD36 expression was not correlated with the prognosis of advanced cervical cancer. E: Kaplan-Meier analysis showed CD36 expression was not correlated with the prognosis of cervical cancer in stage 3. F: Kaplan-Meier analysis showed CD36 expression was not correlated with the prognosis of cervical cancer in stage 4. G, I: The expressions of CD44, CD133, Nanog, YAP, TAZ, MEK5 and ERK5 were increased after enhanced CD36 expression in C33a cells. H, J: The expressions of CD44, CD133, Nanog, YAP, TAZ, MEK5 and ERK5 in HeLa cells were reduced along with the down-regulation of CD36.

0.58) and C33a group (2.33 ± 0.57). The Cell Counting Kit-8 assay revealed that CD36 overexpression significantly enhanced the proliferative capacity of C33a cells (**Figure 3D**). In contrast, the number of spheres larger than 100 μm decreased in the HeLa/siRNA CD36 group (2.33 ± 0.58) compared with the HeLa/NC-siRNA group (5.33 ± 0.57) and HeLa group

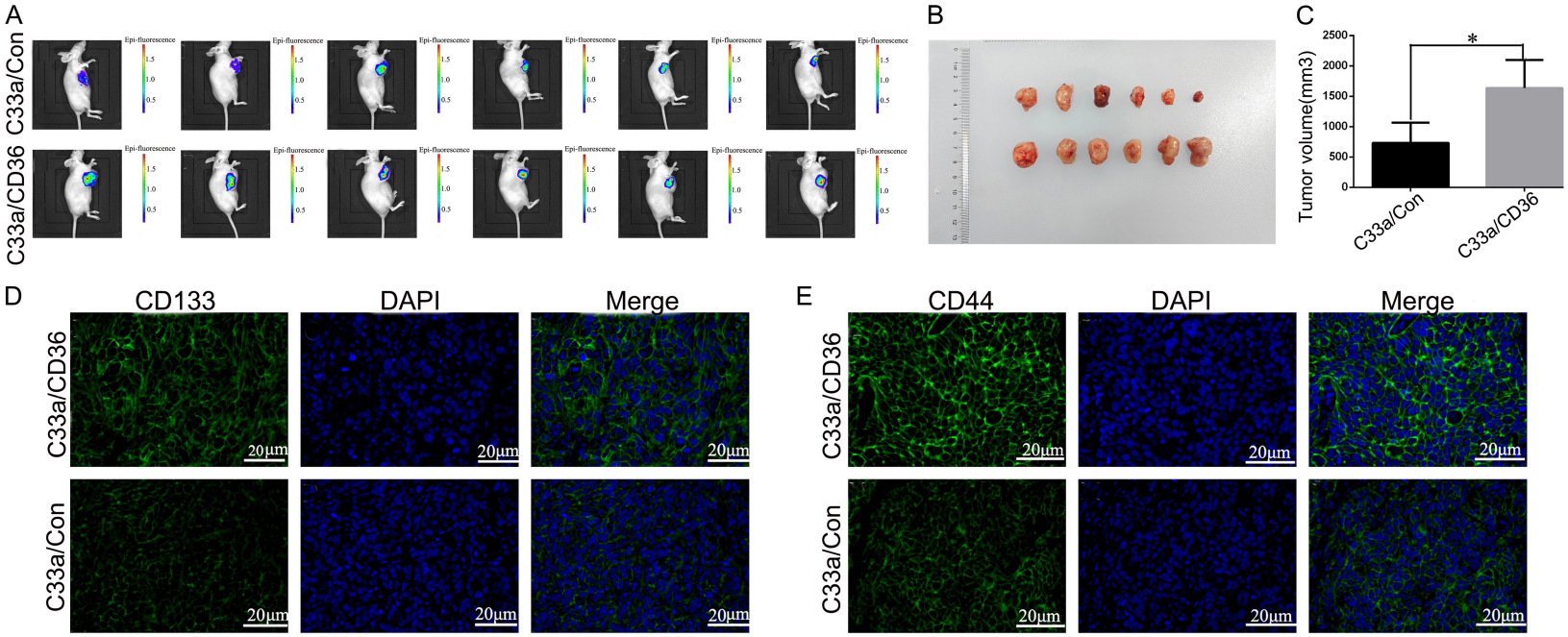

Figure 2. CD36 promotes stemness and tumor growth. A: CD36 over-expression (C33a/CD36 group) promoted tumor growth *in vivo* compared to the control group (C33a/Con group). B: Upper row: C33a/Con group; Lower row: C33a/CD36 group. C: Statistical plots of tumor volume in C33a/CD36 group and C33a/Con group (n=6). D: CD133 expression in C33a/CD36 group was significantly enhanced compared to the C33a/Con group (×400). E: CD44 expression in C33a/CD36 group was significantly enhanced compared to the C33a/Con group (×400).

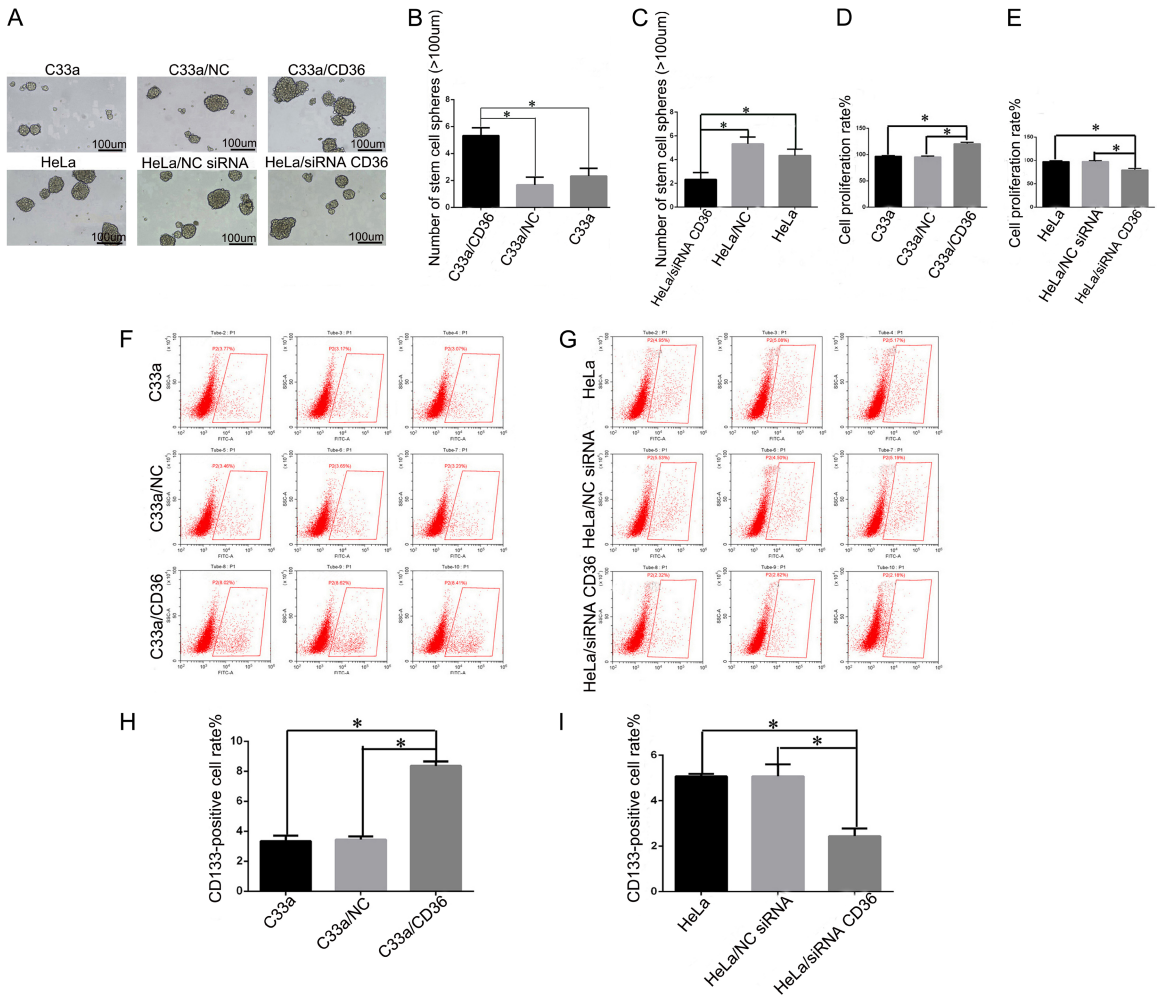

Figure 3. CD36 promotes stemness of cervical cancer cells. (A, B) The number of stem cell spheres with a diameter larger than 100 μm in the C33a/CD36 group was the highest. (A-C) Interfering with CD36 expression in HeLa cells suppressed the number of stem cell spheres larger than 100 μm (A: ×200). (D) The proliferative ability of C33a/CD36 group was increased compared to the C33a and C33a/NC group. (E) Interfering with CD36 expression suppressed the proliferative ability of HeLa cells. (F) The CD133-positive cells in the C33a/CD36 group were the highest compared to the C33a and C33a/NC group. (G) The CD133-positive cells in the HeLa/siRNA CD36 group were the least compared to the HeLa and HeLa/NC siRNA group. (H) Statistical chart of CD133-positive cell rate in C33a, C33a/NC and C33a/CD36 group. (I) Statistical chart of CD133-positive cell rate in HeLa, HeLa/NC siRNA and HeLa/siRNA CD36 group. All experiments were performed in triplicate. *P<0.05.

(4.34 ± 0.54) (**Figure 3A**, **3C**). Proliferation was also reduced in the HeLa/siRNA CD36 group relative to the HeLa/NC-siRNA and HeLa groups (**Figure 3E**). Flow cytometry analysis further demonstrated a higher percentage of CD133-positive cells in the C33a/CD36 group (8.35 ± 0.30%) than in the C33a/NC group (3.45 ± 0.21%) and C33a group (3.33 ± 0.37%) (**Figure 3F**, **3H**). Conversely, fewer CD133-positive cells were observed in the HeLa/siRNA CD36 group (2.44 ± 0.33%) compared to the HeLa/NC-siRNA (5.07 ± 0.11%) and HeLa groups (5.06 ± 0.52%) (**Figure 3G** and **3I**). These findings suggest that CD36 plays a critical role in promoting the stemness of cervical cancer cells *in vitro*.

CD36 overexpression augmented stemness of cervical CSCs

We further sorted CD133-positive C33a cells using flow cytometry and established a CD36-overexpressing cervical cancer stem cell model (C33a-CCSCs/CD36) along with a corresponding control group (C33a-CCSCs/NC). Western blot analysis confirmed that CD36 expression was successfully upregulated in the C33a-CCSCs/CD36 group (**Figure 4A** and **4D**). The

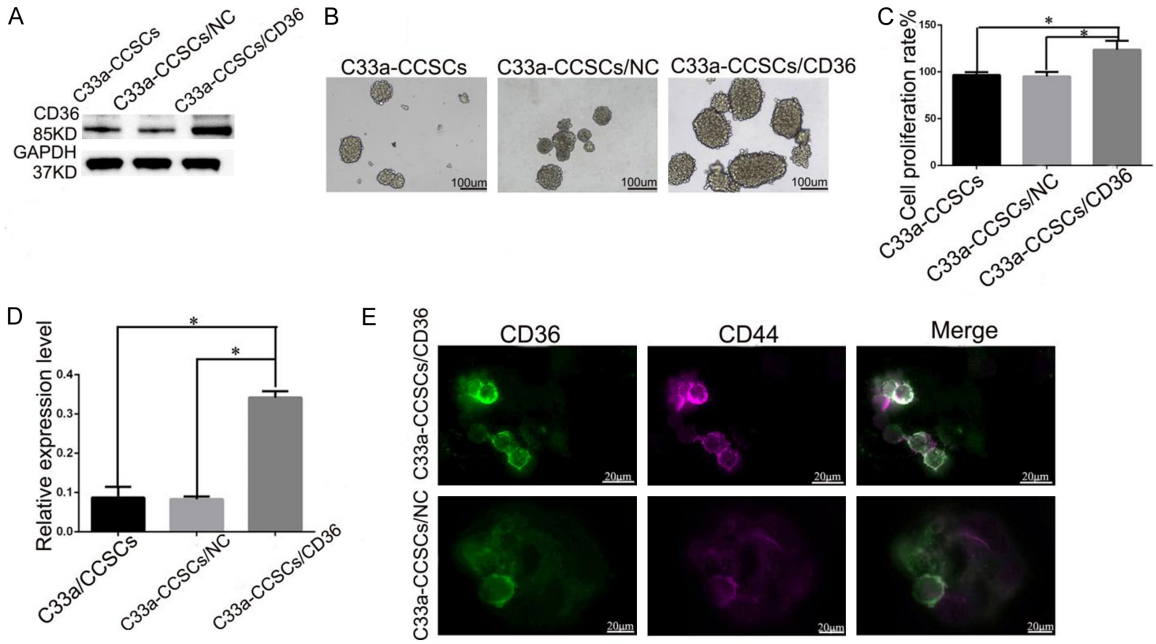

Figure 4. Effect of CD36 overexpression on stemness of cervical cancer stem cells. (A, D) Compared to C33a-CCSCs and C33a-CCSCs/NC, CD36 expression was significantly enhanced in the C33a-CCSCs/CD36 group. (B) The number of stem cell spheres with a diameter larger than 100 μm in C33a-CCSCs/CD36 group was the highest compared to the C33a-CCSCs and C33a-CCSCs/NC group (B: ×200). (C) The proliferative ability of C33a-CCSCs/CD36 group was increased compared to the C33a-CCSCs and C33a-CCSCs/NC group. (E) CD44 expression was increased in C33a-CCSCs/CD36 group compared to C33a-CCSCs/NC group (E: ×400). *P<0.05.

number of stem cell spheres with diameters exceeding 100 μm was significantly higher in the C33a-CCSCs/CD36 group (7.33 ± 0.58) than in the C33a-CCSCs/NC group (3.67 ± 0.58) and the C33a-CCSCs group (3.33 ± 0.57) (**Figure 4B**). Similarly, the proliferative capacity of the C33a-CCSCs/CD36 group was markedly elevated compared with both control groups (**Figure 4C**). Immunofluorescence assays also showed increased CD44 expression in the C33a-CCSCs/CD36 group relative to the C33a-CCSCs/NC group (**Figure 4E**). These findings suggest that CD36 overexpression may enhance the stemness of cervical CSCs.

Elevating CD36 expression potentiated the chemotherapy resistance of cervical CSCs by activating Hippo and MEK5/ERK5 pathways

To further assess whether CD36 expression influences chemotherapy resistance in cervical CSCs, C33a-CCSCs/CD36, C33a-CCSCs/NC, and C33a-CCSCs were treated with 20 μg/ml cisplatin for 24 h. As depicted in **Figure 5A**, the C33a-CCSCs/CD36 group exhibited higher proliferative capacity (130.98 ± 3.15%) compared to the C33a-CCSCs/NC group (97.89 ± 1.28%) and the C33a-CCSCs group (99.57 ± 0.54%). Additionally, the C33a-CCSCs/CD36 group displayed the fewest apoptotic cells relative to the control groups (**Figure 5F**). The expression levels of YAP, TAZ, MEK5, and ERK5 were also elevated in the C33a-CCSCs/CD36 group compared to controls (**Figure 5D**, **5E**).

To further investigate whether the Hippo and MEK5/ERK5 pathways contribute to CD36-regulated chemotherapy resistance in cervical CSCs, C33a-CCSCs/CD36 cells were treated with Verteporfin (a YAP inhibitor) and XMD8-92 (an ERK5 inhibitor). As shown in **Figure 5B**, **5C**, proliferative capacity decreased following treatment with Verteporfin (117.13 ± 1.78% vs. 99.14 ± 0.84%; 99.18 ± 0.47%) or XMD8-92 (120.99 ± 2.32% vs. 99.37 ± 0.74%; 98.43 ± 0.92%) compared to the C33a-CCSCs + cisplatin and C33a-CCSCs/NC + cisplatin groups. Additionally, the number of apoptotic cells in the C33a-CCSCs/CD36 group increased relative to controls after treatment with either inhibitor (**Figure 5G**, **5H**). These findings indicate that CD36 may induce chemotherapy resistance in cervical CSCs through activation of the Hippo and MEK5/ERK5 pathways.

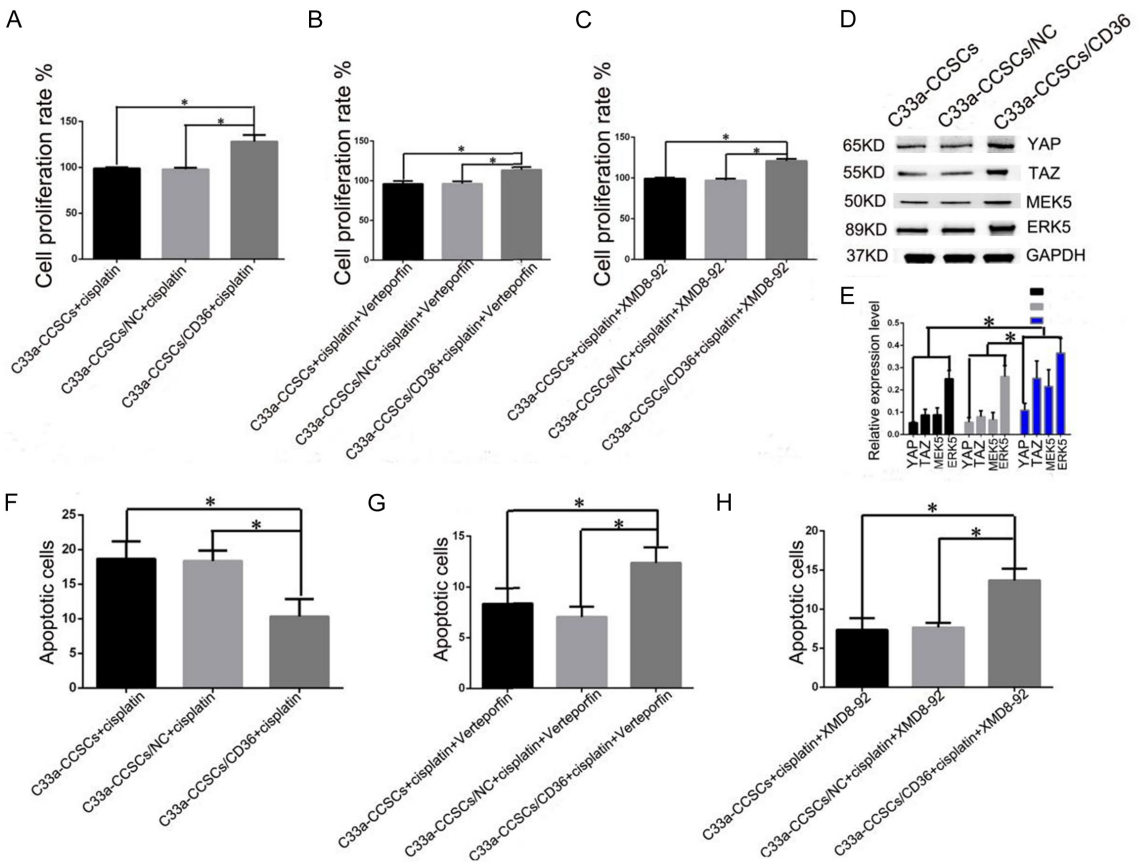

Figure 5. The effects of CD36 expression on chemotherapy resistance of cervical cancer stem cells. A: CD36 promotes proliferative ability of C33a-CCSCs. B, C: Verteporfin and XMD8-92 inhibited proliferation of C33a-CCSCs to some extent. D, E: CD36 increased the expression levels of YAP, TAZ and ERK5. F: CD36 inhibited apoptosis of C33a-CCSCs. G: Verteporfin promotes apoptosis of C33a-CCSCs. H: XMD8-92 promotes apoptosis of C33a-CCSCs. All experiments were performed in triplicate. *P<0.05.

Interfering CD36 expression alleviated the chemotherapy resistance of cervical cancer cells

Conversely, we downregulated CD36 expression in HeLa cells and treated them with 20 μg/ml cisplatin for 24 hours. The colony formation assay revealed fewer colonies in the HeLa/siRNA CD36 group (106.67 ± 14.57) compared with the HeLa/NC siRNA group (161.33 ± 8.08) and HeLa group (148.33 ± 10.02) (**Figure 6A**). The proliferative capacity of the HeLa/siRNA CD36 group (75.10 ± 3.12%) was significantly reduced relative to the HeLa group (94.15 ± 1.18%) and HeLa/NC-siRNA group (97.48 ± 2.57%) (**Figure 6B**). The HeLa/siRNA CD36 group also exhibited the highest number of apoptotic cells (35.28 ± 1.15% vs. 21.27 ± 0.88%; 21.26 ± 0.67%) (**Figure 6C**, **6E**). Furthermore, Bcl-2 expression was decreased, Bax expression increased, and cleaved caspase-3 activity enhanced in the HeLa/siRNA CD36 group, consistent with CD36 downregulation (**Figure 6D**, **6F**). These findings indicate that silencing CD36 inhibits proliferation and promotes apoptosis in HeLa cells following cisplatin treatment. Additionally, the expression of CD44, CD133, and Nanog was significantly reduced in the HeLa/siRNA CD36 group compared with controls (**Figure 6D**, **6F**), suggesting that CD36 knockdown may alleviate chemotherapy resistance by suppressing cervical cancer cell stemness.

Discussion

Previous studies have shown that CD36 promotes the progression and metastasis of oral cancer by facilitating the uptake of exogenous fatty acids [11]. Our prior work also demonstrated that CD36 accelerates epithelial-mesenchymal transition and metastasis in cervical cancer [30]. Additionally, CD36-driven lipid

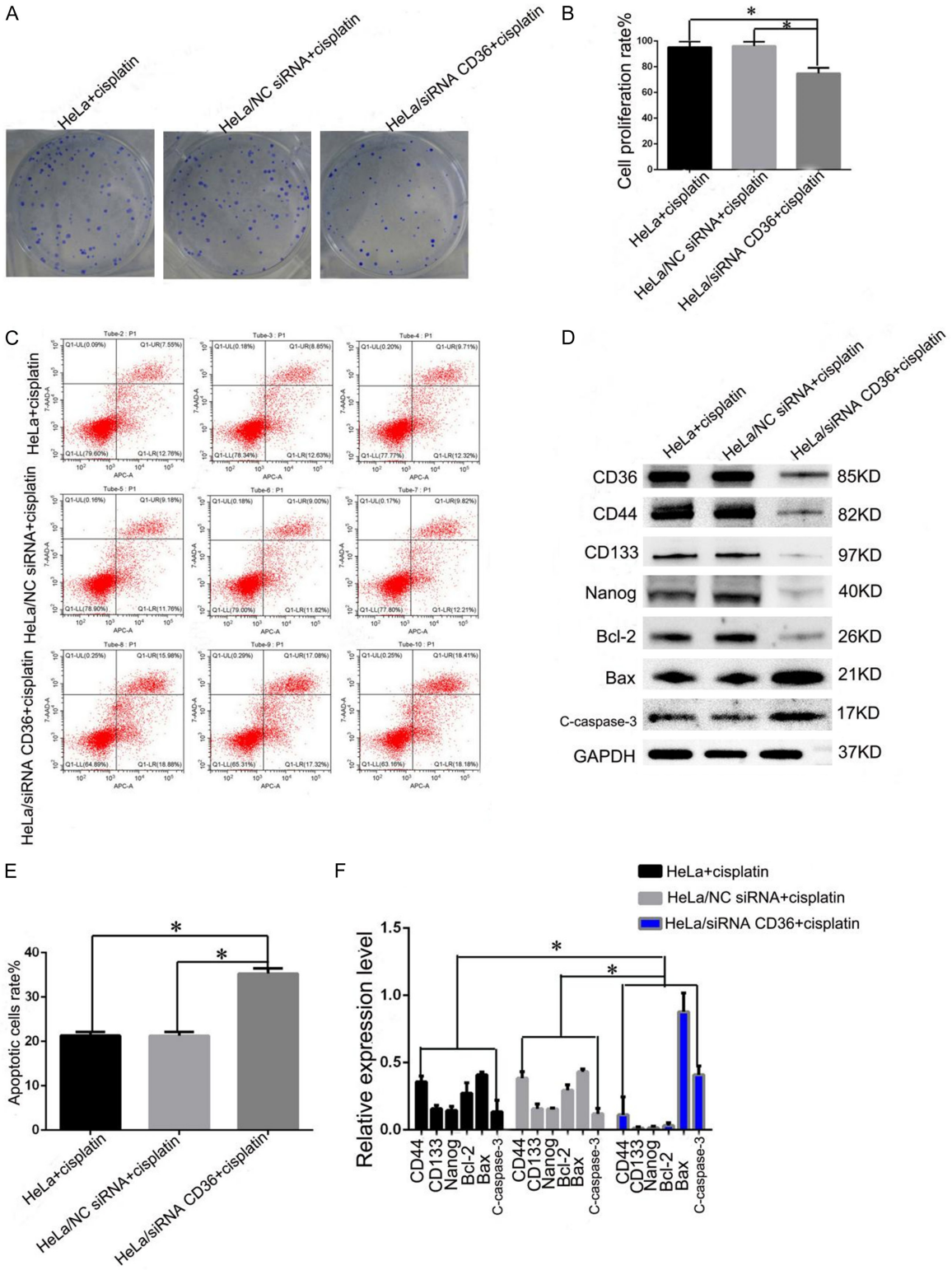

Figure 6. Effects of interfering with CD36 expression on chemotherapy resistance of Hela cells. A: Interfering CD36 expression inhibited clone formation ability of HeLa cells after treatment with cisplatin. B: Interfering with CD36 expression inhibited proliferative ability of HeLa cells after treatment with cisplatin. C, E: Interfering with CD36 expression promoted apoptosis of HeLa cells after treatment with cisplatin. D, F: Compared to control groups, expression of CD44, CD133, Nanog, and Bcl-2 were decreased, and expression of Bax and Caspase-3 were increased in the HeLa/siRNA CD36 group. All experiments were performed in triplicate. *P<0.05.

uptake contributes to chemotherapy resistance. In acute myeloid leukemia, the CD36-fatty acid oxidation (FAO)-oxidative phosphorylation (OXPHOS) axis underlies resistance to chemotherapy [31]. In this study, we investigated the roles of CD36 in regulating stemness and chemotherapy resistance in cervical cancer cells.

We found that CD36 promoted the formation of larger stem cell spheres and enhanced the expression of stem cell markers. Additionally, both the proliferative capacity and sphere-forming ability increased following CD36 transfection in C33a-CCSCs. Similarly, Gyamfi et al. reported that CD36 knockdown reduced stemness marker expression in breast cancer cells [32]. Collectively, these results demonstrate that CD36 promotes the stemness of cervical cancer cells.

Chemotherapy resistance is a major factor limiting the clinical efficacy of cervical cancer treatment. Bioinformatic analysis revealed that CD36 expression was positively correlated with cisplatin resistance in advanced cervical cancer. Therefore, we investigated the role of CD36 in chemotherapy resistance. CD36 overexpression enhanced proliferation and reduced apoptosis in C33a-CCSCs treated with cisplatin. In contrast, CD36 silencing decreased colony formation and proliferation in HeLa cells while increasing apoptosis. These findings suggest that CD36 plays a key role in promoting chemotherapy resistance in cervical cancer cells.

CD44 is a well-established cancer stem cell marker and a key regulator of epithelial-mesenchymal transition [33]. We found that CD36 enhances CD44 expression both *in vitro* and *in vivo*, thereby promoting the stemness of cervical cancer cells. The ERK5 and Hippo pathways are also recognized as important contributors to chemotherapy resistance and stemness in cancer cells [34-37]. YAP, a central effector of the Hippo pathway, promotes immune evasion in BRAF inhibitor-resistant melanoma by upregulating PD-L1 [38], while the MEK5-ERK5 -STAT3 axis accelerates self-renewal and tumorigenicity in glioma stem cells [39]. In our study, CD36 upregulated the expression of YAP, TAZ, MEK5, and ERK5, thereby activating both the Hippo and ERK5 pathways. Vittoria et al. reported that Hippo pathway activation is mediated through mitogen-activated protein kinase (MAPK) signaling [40], and CD36 has been shown to activate MAPK signaling [41]. Thus, we speculate that CD36 may activate the Hippo pathway via MAPK activation. Moreover, treatment with YAP and ERK5 inhibitors reduced proliferation and increased apoptosis in C33a-CCSCs/CD36 cells, further supporting the involvement of the Hippo and ERK5 pathways in CD36-mediated chemotherapy resistance.

In summary, our findings demonstrate that CD36 promotes stemness and chemotherapy resistance in cervical cancer cells. Notably, CD44, Hippo, and MEK5/ERK5 pathways are involved in CD36-mediated resistance and contribute to enhanced stemness. Collectively, these results suggest that CD36 may be a promising therapeutic target for improving the prognosis of cervical cancer.

Acknowledgements

This project was funded by a grant from Shenzhen Science and Technology Program (JCYJ20220530144407017) and Guangdong Provincial Basic and Applied Basic Research Foundation Project (2025A1515011028).

Disclosure of conflict of interest

None.

Address correspondence to: Chao Zeng, Department of Pathology, The Eighth Affiliated Hospital, Sun Yat-sen University, No. 3025 Shennan Middle Road, Futian District, Shenzhen 518033, Guangdong, China. E-mail: zengch35@mail.sysu.edu.cn

References

[1] Arbyn M, Weiderpass E, Bruni L, de Sanjosé S, Saraiya M, Ferlay J and Bray F. Estimates of incidence and mortality of cervical cancer in 2018: a worldwide analysis. Lancet Glob Health 2020; 8: 191-203.

[2] Wu P, Xiong H, Yang M, Li L, Wu P, Lazare C, Cao C, Gao P, Meng Y, Zhi W, Lin S, Hu J, Wei J, Ma D, Liu J, Yin P and Xing H. Co-infections of HPV16/18 with other high-risk HPV types and the risk of cervical carcinogenesis: a large population-based study. Gynecol Oncol 2019; 155: 436-443.

[3] Sundström K, Eloranta S, Sparén P, Arnheim Dahlström L, Gunnell A, Lindgren A, Palmgren J, Ploner A, Sanjeevi CB, Melbye M, Dillner J, Adami HO and Ylitalo N. Prospective study of human papillomavirus (HPV) types, HPV per-

sistence, and risk of squamous cell carcinoma of the cervix. Cancer Epidemiol Biomarkers Prev 2010; 19: 2469-2478.
[4] Ferrandina G, Lauriola L, Distefano MG, Zannoni GF, Gessi M, Legge F, Maggiano N, Mancuso S, Capelli A, Scambia G and Ranelletti FO. Increased cyclooxygenase-2 expression is associated with chemotherapy resistance and poor survival in cervical cancer patients. J Clin Oncol 2002; 20: 973-981.
[5] Martin C, Chevrot M, Poirier H, Passilly-Degrace P, Niot I and Besnard P. CD36 as a lipid sensor. Physiol Behav 2011; 105: 36-42.
[6] Hale JS, Otvos B, Sinyuk M, Alvarado AG, Hitomi M, Stoltz K, Wu Q, Flavahan W, Levison B, Johansen ML, Schmitt D, Neltner JM, Huang P, Ren B, Sloan AE, Silverstein RL, Gladson CL, DiDonato JA, Brown JM, McIntyre T, Hazen SL, Horbinski C, Rich JN and Lathia JD. Cancer stem cell-specific scavenger receptor CD36 drives glioblastoma progression. Stem Cells 2014; 32: 1746-1758.
[7] Zhao J, Zhi Z, Wang C, Xing H, Song G, Yu X, Zhu Y, Wang X, Zhang X and Di Y. Exogenous lipids promote the growth of breast cancer cells via CD36. Oncol Rep 2017; 38: 2105-2115.
[8] Zhou X, Su M, Lu J, Li D, Niu X and Wang Y. CD36: the bridge between lipids and tumors. Molecules 2024; 29: 531.
[9] Ladanyi A, Mukherjee A, Kenny HA, Johnson A, Mitra AK, Sundaresan S, Nieman KM, Pascual G, Benitah SA, Montag A, Yamada SD, Abumrad NA and Lengyel E. Adipocyte-induced CD36 expression drives ovarian cancer progression and metastasis. Oncogene 2018; 37: 2285-2301.
[10] Liu H, Guo W, Wang T, Cao P, Zou T, Peng Y, Yan T, Liao C, Li Q, Duan Y, Han J, Zhang B, Chen Y, Zhao D and Yang X. CD36 inhibition reduces non-small-cell lung cancer development through AKT-mTOR pathway. Cell Biol Toxicol 2024; 40: 10.
[11] Pascual G, Avgustinova A, Mejetta S, Martín M, Castellanos A, Attolini CS, Berenguer A, Prats N, Toll A, Hueto JA, Bescós C, Di Croce L and Benitah SA. Targeting metastasis-initiating cells through the fatty acid receptor CD36. Nature 2017; 541: 41-45.
[12] Wang H, Liu F, Wu X, Zhu G, Tang Z, Qu W, Zhao Q, Huang R, Tian M, Fang Y, Jiang X, Tao C, Gao J, Liu W, Zhou J, Fan J, Wu D and Shi Y. Cancer-associated fibroblasts contributed to hepatocellular carcinoma recurrence and metastasis via CD36-mediated fatty-acid metabolic reprogramming. Exp Cell Res 2024; 435: 113947.
[13] Zhu GQ, Tang Z, Huang R, Qu WF, Fang Y, Yang R, Tao CY, Gao J, Wu XL, Sun HX, Zhou YF, Song SS, Ding ZB, Dai Z, Zhou J, Ye D, Wu DJ, Liu WR, Fan J and Shi YH. CD36^{+} cancer-associated fibroblasts provide immunosuppressive microenvironment for hepatocellular carcinoma via secretion of macrophage migration inhibitory factor. Cell Discov 2023; 9: 25.
[14] Liao M, Li Y, Xiao A, Lu Q, Zeng H, Qin H, Zheng E, Luo X, Chen L, Ruan XZ, Yang P and Chen Y. HIF-2α-induced upregulation of CD36 promotes the development of CCRCC. Exp Cell Res 2022; 421: 113389.
[15] Liu LZ, Wang B, Zhang R, Wu Z, Huang Y, Zhang X, Zhou J, Yi J, Shen J, Li MY and Dong M. The activated CD36-Src axis promotes lung adenocarcinoma cell proliferation and actin remodeling-involved metastasis in high-fat environment. Cell Death Dis 2023; 14: 548.
[16] Luo X, Zheng E, Wei L, Zeng H, Qin H, Zhang X, Liao M, Chen L, Zhao L, Ruan XZ, Yang P and Chen Y. The fatty acid receptor CD36 promotes HCC progression through activating Src/PI3K/AKT axis-dependent aerobic glycolysis. Cell Death Dis 2021; 12: 328.
[17] Pan J, Fan Z, Wang Z, Dai Q, Xiang Z, Yuan F, Yan M, Zhu Z, Liu B and Li C. CD36 mediates palmitate acid-induced metastasis of gastric cancer via AKT/GSK-3β/β-catenin pathway. J Exp Clin Cancer Res 2019; 38: 52.
[18] Tao L, Ding X, Yan L, Xu G, Zhang P, Ji A and Zhang L. CD36 accelerates the progression of hepatocellular carcinoma by promoting FAs absorption. Med Oncol 2022; 39: 202.
[19] Yang L, Sun J, Li M, Long Y, Zhang D, Guo H, Huang R and Yan J. Oxidized low-density lipoprotein links hypercholesterolemia and bladder cancer aggressiveness by promoting cancer stemness. Cancer Res 2021; 81: 5720-5732.
[20] Bao S, Wu Q, McLendon RE, Hao Y, Shi Q, Hjelmeland AB, Dewhirst MW, Bigner DD and Rich JN. Glioma stem cells promote radioresistance by preferential activation of the DNA damage response. Nature 2006; 444: 756-60.
[21] Lopez-Ayllon BD, Moncho-Amor V, Abarrategi A, Ibañez de Cáceres I, Castro-Carpeño J, Belda-Iniesta C, Perona R and Sastre L. Cancer stem cells and cisplatin-resistant cells isolated from non-small-lung cancer cell lines constitute related cell populations. Cancer Med 2014; 3: 1099-1111.
[22] Srivastava AK, Han C, Zhao R, Cui T, Dai Y, Mao C, Zhao W, Zhang X, Yu J and Wang QE. Enhanced expression of DNA polymerase eta contributes to cisplatin resistance of ovarian cancer stem cells. Proc Natl Acad Sci U S A 2015; 112: 4411-4416.
[23] Zhang J, Chen X, Bian L, Wang Y and Liu H. CD44^{+}/CD24^{+}-expressing cervical cancer cells

and radioresistant cervical cancer cells exhibit cancer stem cell characteristics. Gynecol Obstet Invest 2019; 84: 174-182.
[24] Li S, Li X, Yang YB and Wu SF. YAP/TAZ-TEAD activity promotes the malignant transformation of cervical intraepithelial neoplasia through enhancing the characteristics and Warburg effect of cancer stem cells. Apoptosis 2024; 29: 1198-1210.
[25] Yang W, Soares J, Greninger P, Edelman EJ, Lightfoot H, Forbes S, Bindal N, Beare D, Smith JA, Thompson IR, Ramaswamy S, Futreal PA, Haber DA, Stratton MR, Benes C, McDermott U and Garnett MJ. Genomics of Drug Sensitivity in Cancer (GDSC): a resource for therapeutic biomarker discovery in cancer cells. Nucleic Acids Res 2013; 41: D955-961.
[26] Zhu Y, Meng X, Ruan X, Lu X, Yan F and Wang F. Characterization of neoantigen load subgroups in gynecologic and breast cancers. Front Bioeng Biotechnol 2020; 13: 702.
[27] Huang da W, Sherman BT and Lempicki RA. Systematic and integrative analysis of large gene lists using DAVID bioinformatics resources. Nat Protoc 2009; 4: 44-57.
[28] Wang P, Wang Y, Hang B, Zou X and Mao JH. A novel gene expression-based prognostic scoring system to predict survival in gastric cancer. Oncotarget 2016; 7: 55343-55351.
[29] Zeng C, Ke Z, Song Y, Yao Y, Hu X, Zhang M, Li H and Yin J. Annexin A3 is associated with a poor prognosis in breast cancer and participates in the modulation of apoptosis in vitro by affecting the Bcl-2/Bax balance. Exp Mol Pathol 2013; 95: 23-31.
[30] Deng M, Cai X, Long L, Xie L, Ma H, Zhou Y, Liu S and Zeng C. CD36 promotes the epithelial-mesenchymal transition and metastasis in cervical cancer by interacting with TGF-beta. J Transl Med 2019; 17: 352.
[31] Farge T, Saland E, de Toni F, Aroua N, Hosseini M, Perry R, Bosc C, Sugita M, Stuani L, Fraisse M, Scotland S, Larrue C, Boutzen H, Féliu V, Nicolau-Travers ML, Cassant-Sourdy S, Broin N, David M, Serhan N, Sarry A, Tavitian S, Kaoma T, Vallar L, Iacovoni J, Linares LK, Montersino C, Castellano R, Griessinger E, Collette Y, Duchamp O, Barreira Y, Hirsch P, Palama T, Gales L, Delhommeau F, Garmy-Susini BH, Portais JC, Vergez F, Selak M, Danet-Desnoyers G, Carroll M, Récher C and Sarry JE. Chemotherapy-resistant human acute myeloid leukemia cells are not enriched for leukemic stem cells but require oxidative metabolism. Cancer Discov 2017; 7: 716-735.
[32] Gyamfi J, Yeo JH, Kwon D, Min BS, Cha YJ, Koo JS, Jeong J, Lee J and Choi J. Interaction between CD36 and FABP4 modulates adipocyte-induced fatty acid import and metabolism in breast cancer. NPJ Breast Cancer 2021; 7: 129.
[33] Hassn Mesrati M, Syafruddin SE, Mohtar MA and Syahir A. CD44: a multifunctional mediator of cancer progression. Biomolecules 2021; 11: 1850.
[34] Pereira DM, Gomes SE, Borralho PM and Rodrigues CMP. MEK5/ERK5 activation regulates colon cancer stem-like cell properties. Cell Death Discov 2019; 5: 68.
[35] Song R, Gu D, Zhang L, Zhang X, Yu B, Liu B and Xie J. Functional significance of Hippo/YAP signaling for drug resistance in colorectal cancer. Mol Carcinog 2018; 57: 1608-1615.
[36] Sa P, Singh P, Panda S, Swain RK, Dash R and Sahoo SK. Reversal of cisplatin resistance in oral squamous cell carcinoma by piperlongumine loaded smart nanoparticles through inhibition of Hippo-YAP signaling pathway. Transl Res 2024; 268: 63-78.
[37] Lambrescu IM, Gaina GF, Ceafalan LC and Hinescu ME. Inside anticancer therapy resistance and metastasis. Focus on CD36. J Cancer 2024; 15: 1675-86.
[38] Nguyen CDK and Yi C. YAP/TAZ Signaling and resistance to cancer therapy. Trends Cancer 2019; 5: 283-296.
[39] Fukasawa K, Lyu J, Kubo T, Tanaka Y, Suzuki A, Horie T, Tomizawa A, Osumi R, Iwahashi S, Tokumura K, Murata M, Kobayashi M, Todo T, Hirao A and Hinoi E. MEK5-ERK5 axis promotes self-renewal and tumorigenicity of glioma stem cells. Cancer Res Commun 2023; 3: 148-159.
[40] Vittoria MA, Kingston N, Kotynkova K, Xia E, Hong R, Huang L, McDonald S, Tilston-Lunel A, Darp R, Campbell JD, Lang D, Xu X, Ceol CJ, Varelas X and Ganem NJ. Inactivation of the Hippo tumor suppressor pathway promotes melanoma. Nat Commun 2022; 13: 3732.
[41] Nan P, Dong X, Bai X, Lu H, Liu F, Sun Y and Zhao X. Tumor-stroma TGF-β1-THBS2 feedback circuit drives pancreatic ductal adenocarcinoma progression via integrin αvβ3/CD36-mediated activation of the MAPK pathway. Cancer Lett 2022; 528: 59-75.

Table S1. The transcriptome sequencing data of 62 advanced cervical cancer samples

gene	time	OS	Stage	CD36	status
TCGA-JX-A3Q0-01A	212.5	0	Stage III	0.106334	0
TCGA-VS-A9UD-01A	24.63333	0	Stage IIIA	0.379796	0
TCGA-VS-A950-01A	40.7	0	Stage IIIA	3.011863	1
TCGA-LP-A5U2-01A	0.3	0	Stage IIIB	0.072316	0
TCGA-C5-A1BQ-01C	20.13333	1	Stage IIIB	0.079746	0
TCGA-FU-A40J-01A	14.2	0	Stage IIIB	0.11357	0
TCGA-DR-A0ZM-01A	59.7	0	Stage IIIB	0.118669	0
TCGA-DG-A2KJ-01A	96.43333	0	Stage IIIB	0.154352	0
TCGA-FU-A23K-01A	12.4	0	Stage IIIB	0.200696	0
TCGA-C5-A7X3-01A	9.466667	1	Stage IIIB	0.269161	0
TCGA-BI-A0VR-01A	50.16667	0	Stage IIIB	0.340719	0
TCGA-FU-A77O-01A	1.133333	0	Stage IIIB	0.380776	0
TCGA-EK-A2PI-01A	19.53333	0	Stage IIIB	0.397804	0
TCGA-C5-A1MN-01A	41.5	1	Stage IIIB	0.427787	0
TCGA-DG-A2KK-01A	83.2	0	Stage IIIB	0.457832	0
TCGA-VS-A8EC-01A	47.16667	0	Stage IIIB	0.490488	0
TCGA-EA-A6QX-01A	24.33333	0	Stage IIIB	0.498557	0
TCGA-LP-A4AU-01A	11.43333	0	Stage IIIB	0.530072	0
TCGA-C5-A1BI-01B	37.06667	0	Stage IIIB	0.55122	0
TCGA-EK-A3GN-01A	0.9	0	Stage IIIB	0.55288	0
TCGA-VS-A9UL-01A	14.73333	1	Stage IIIB	0.605414	1
TCGA-MA-AA43-01A	11.53333	0	Stage IIIB	0.610311	1
TCGA-ZX-AA5X-01A	3.966667	0	Stage IIIB	0.765881	1
TCGA-C5-A7UH-01A	132.9333	0	Stage IIIB	0.779847	1
TCGA-EA-A3QD-01A	13.23333	0	Stage IIIB	0.958895	1
TCGA-C5-A1MH-01A	39.53333	1	Stage IIIB	1.105976	1
TCGA-EK-A2GZ-01A	12.76667	0	Stage IIIB	1.20161	1
TCGA-VS-A954-01A	57.13333	0	Stage IIIB	1.286538	1
TCGA-FU-A3TQ-01A	26.5	0	Stage IIIB	1.364193	1
TCGA-HM-A4S6-01A	15.13333	0	Stage IIIB	1.602762	1
TCGA-DS-A3LQ-01A	23.3	0	Stage IIIB	1.664361	1
TCGA-MA-AA3X-01A	19.83333	0	Stage IIIB	2.007529	1
TCGA-UC-A7PG-01A	12.33333	1	Stage IIIB	2.123608	1
TCGA-EA-A44S-01A	12.3	0	Stage IIIB	2.133504	1
TCGA-C5-A1MK-01A	2.466667	1	Stage IIIB	2.269569	1
TCGA-FU-A5XV-01A	10.7	0	Stage IIIB	2.381891	1
TCGA-VS-A8EB-01A	10.16667	1	Stage IIIB	2.912379	1
TCGA-EK-A2PL-01A	0.433333	0	Stage IIIB	3.820598	1
TCGA-C5-A2LZ-01A	101.5333	1	Stage IIIB	4.217823	1
TCGA-C5-A7CL-01A	15.7	1	Stage IIIB	4.889445	1
TCGA-VS-A8EH-01A	32.86667	0	Stage IIIB	6.708641	1
TCGA-VS-A953-01A	15.9	1	Stage IVA	0.070301	0
TCGA-VS-A9V4-01A	4.4	1	Stage IVA	0.21431	0
TCGA-C5-A7CK-01A	136.2	1	Stage IVA	0.324765	0
TCGA-VS-A8QC-01A	11.66667	1	Stage IVA	0.463472	0
TCGA-VS-A9UH-01A	47.56667	0	Stage IVA	0.726318	1
TCGA-VS-A9UV-01A	3.466667	1	Stage IVA	0.823503	1

TCGA-DS-A1O9-01A	8.866667	1	Stage IVA	1.211253	1
TCGA-VS-A8EK-01A	27.63333	1	Stage IVA	2.647716	1
TCGA-EA-A50E-01A	7.566667	1	Stage IVA	4.472247	1
TCGA-VS-A9V1-01A	5.233333	1	Stage IVB	0.076624	0
TCGA-IR-A3LI-01A	83.1	0	Stage IVB	0.089749	0
TCGA-EX-A449-01A	14.9	0	Stage IVB	0.100071	0
TCGA-EK-A2RB-01A	0.3	0	Stage IVB	0.158049	0
TCGA-C5-A7X5-01A	13.8	1	Stage IVB	0.238642	0
TCGA-VS-A9UY-01A	18.5	1	Stage IVB	0.332576	0
TCGA-VS-A9UM-01A	27.63333	1	Stage IVB	0.444087	0
TCGA-VS-A9U6-01A	44	0	Stage IVB	0.485612	0
TCGA-HM-A6W2-01A	9.566667	0	Stage IVB	0.935705	1
TCGA-VS-A8QM-01A	31.7	1	Stage IVB	1.552829	1
TCGA-JW-A5VH-01A	3.333333	1	Stage IVB	3.769822	1
TCGA-VS-A9V3-01A	18	0	Stage IVB	6.390622	1